RSC Pharmaceutics

ROYAL SOCIETY OF CHEMISTRY

PAPER

View Article Online
View Journal

Open Access Article. Published on 12 January 2026. Downloaded on 3/17/2026 6:44:35 PM.
This article is licensed under a Creative Commons Attribution-NonCommercial 3.0 Unported Licence.

Check for updates

Cite this: DOI: 10.1039/d5pm00267b

Extraction, characterization and evaluation of jute (*Corchorus olitorius*) leaf polysaccharide as a binding agent for matrix tablet formulation

Olivia Sen,[a,b] Devlina Pal,*[a] Tamal Jana,[b] Sanchita Das,*[c] Gouranga Nandi[d] and Sreejan Manna *[b]

The objective of the present investigation was to estimate the potential of jute (*Corchorus olitorius*) leaf polysaccharide (JLP) as a tablet binder. This polysaccharide was extracted by a simple decoction method using distilled water and precipitated with twice the volume of acetone. The extracted JLP was dried, powdered and subjected to several characterizations, such as FTIR spectroscopy, DSC, XRD, scanning electron microscopy, zeta potential analysis, particle size analysis, tests for the presence of phytochemical constituents, elemental analysis, and stability study in an aqueous environment, along with characterizing other physicochemical properties. Diclofenac sodium-incorporated granules were prepared using 2.5%, 5%, 7.5% and 10% w/w JLP concentrations, and the prepared granules were evaluated and compressed into tablets. The formulated tablet batches were evaluated for disintegration, drug release and kinetics study. The obtained results were compared with those of similar concentrations of starch and PVP K-30 batches used as tablet binders. Results of FTIR spectroscopy and DSC study established the compatibility between JLP and diclofenac sodium (DS) in the formulation. SEM analysis indicated that drug release from the tablet matrix was predominantly controlled by surface erosion and pore development, which facilitated dissolution. JLP formulations revealed a drug release of >75% at 45 min (77.75% ± 1.298% to 87.352% ± 1.35%). The Korsmeyer–Peppas release exponent (n) from 0.56 to 0.84 indicated that the majority of batches exhibited anomalous (non-Fickian) transport, signifying that drug release was influenced by both diffusion and polymer relaxation or erosion. Preliminary study findings established JLP as a suitable pharmaceutical excipient. Even at 2.5% binder concentration, low friability (0.308% ± 0.057%), hardness (4.22 ± 0.105 kg m^{-2}) and drug release pattern of the prepared tablets indicated the potential of the extracted novel JLP as a sustainable and safe alternative to conventional tablet binders.

Received 30th September 2025,
Accepted 17th December 2025

DOI: 10.1039/d5pm00267b

rsc.li/RSCPharma

1. Introduction

As the most stable dosage form and the one most preferred by patients, tablets have outnumbered other dosage forms in terms of consumption worldwide.[1] The lowest content variability, highest precision in dose and flexibility in designing and manufacturing have also made tablets favourable to formulation scientists. In tablet manufacturing, wet granulation techniques are widely employed due to their suitability and adaptability to a vast number of excipients.[2,3] The incorporation of binding agents plays a very important role in the performance of the developed tablets. The selection of the binding agent in optimum concentration during wet granulation is crucial as it can impart plasticity, increase the flow characteristics and compressibility of the prepared granules, and aid in increasing interparticulate cohesive force alongside mechanical strength.[4] Besides the incorporation of synthetic and semisynthetic binders in pharmaceutical tablet manufacturing, naturally occurring binders are increasingly gaining the attention of pharmaceutical researchers.[5] Among natural polymers, polysaccharides are preferred due to their excellent biocompatibility, biodegradation profile, easy availability and binding potential at lower concentrations.[6] This has enhanced the quest to explore newer polysaccharides as binding agents for tablet preparation.[7]

Many naturally occurring polysaccharides, including starch, acacia, sodium alginate, and tragacanth, have been widely employed as tablet binders for a long time. Recent investigations have reported the incorporation of many novel polysac-

[a]Department of Pharmaceutical Technology, JIS University, Agarpara, Kolkata, West Bengal 700109, India. E-mail: devlina.pal2017@gmail.com
[b]Department of Pharmaceutical Technology, Brainware University, Barasat, Kolkata, West Bengal-700125, India. E-mail: manna.sreejan@gmail.com
[c]Department of Pharmaceutical Technology, B.C.D.A. College of Pharmacy & Technology, Hridaypur, Barasat, Kolkata, West Bengal 700127, India. E-mail: sanchitadasbhowmik@gmail.com
[d]Department of Pharmaceutical Technology, University of North Bengal, Raja Rammohunpur, Dist., Darjeeling, West Bengal, 734013, India

Open Access Article. Published on 12 January 2026. Downloaded on 3/17/2026 6:44:35 PM.
This article is licensed under a Creative Commons Attribution-NonCommercial 3.0 Unported Licence.

charides as binding agents in tablet manufacturing. These include taro stolon polysaccharide, fenugreek gum, and guar gum. Polysaccharides from edible sources have become a recent highlight in pharmaceutical research due to their proven biocompatibility, edible nature and assured biodegradation.[8–11] In the quest for sustainable development of alternative resources of pharmaceutical excipients, we explored the potential of jute leaf polysaccharide (JLP) as a binder for pharmaceutical tablet preparation. Jute (*Corchorus olitorius*) is a commonly cultivated vegetable across the world.[12] It belongs to the family Malvaceae.[13] Although it is mainly cultivated as a fiber crop and has found extensive application in the packaging and textile industry, jute leaves are known to be a commonly consumed vegetable in many parts of Africa and Asia. This annual herbaceous plant usually grows in hot and humid climates with sufficient rainfall. The leaves of the jute plant contain polysaccharides.[14] The JLP has not been reported as a pharmaceutical excipient in any type of dosage form. In this investigation, we extracted jute leaf polysaccharides from jute leaves and explored their binding ability in tablet preparation using diclofenac sodium (DS) as a model drug.

DS is a commonly used non-steroidal anti-inflammatory drug that is widely prescribed in the therapy of arthritis.[15] This analgesic and antipyretic drug requires multiple dosing (3 to 4 times a day) due to its short biological half-life of 2 h.[16] It shows good solubility in an alkaline medium.[17] The present investigation aimed to assess the potential of JLP as a binding agent in the formation of matrix tablets using DS as a model drug. Additionally, we characterized a novel JLP as a pharmaceutical excipient. The characterization techniques include phytoconstituent screening, organoleptic properties, total polysaccharide content, ^{13}C solid-state NMR spectroscopy analysis, elemental analysis, FTIR spectroscopy, molar mass, zeta potential, particle size, pH, surface tension, viscosity, water solubility, swelling index, DSC, TGA, DTA, powder X-ray diffraction, and scanning electron microscopy. The preformulation study confirmed drug–excipient compatibility; therefore, DS-incorporated granules were prepared and evaluated before compression into tablets. The prepared JLP-based tablets were evaluated and compared with other conventionally used binding agents: starch and PVP K-30.

2. Materials and methods

2.1 Materials

JLP was extracted from fresh jute leaves collected from the local market in the District of North 24 PGS, West Bengal, India, from June to August 2024. DS was obtained commercially from TCI, India. Acetone, ethanol, starch, and PVP K-30 were obtained from Merck, India. Acacia, lactose monohydrate, magnesium stearate, and refined talc were bought from SD Fine Chemicals, India. All chemicals and reagents employed were of analytical grade. All experiments were conducted using triple-distilled water.

2.2 Methods

2.2.1 Extraction and purification of JLP. Extraction and purification of jute leaf polysaccharides were performed using the method described by Oh *et al.*, with a slight modification.[18] Jute leaf polysaccharides were extracted from freshly collected jute leaves. The collected species of the jute plant were authenticated by the Botanical Survey of India, Shibpur, Howrah, India. The fresh jute leaves were first washed thoroughly with tap water, then rinsed with distilled water and cut into small pieces. A measured quantity of leaves was placed in a glass beaker containing distilled water and boiled in a water bath for 2 h at 70 °C with intermittent stirring. Then, it was allowed to cool to room temperature, and the mucilaginous liquid was filtered through a muslin cloth. The supernatant was collected following centrifugation of the liquid extract at 2500 rpm for 20 minutes. Ethyl alcohol was added into the supernatant to attain a final concentration of 55% v/v for the precipitation of mucilage. Subsequently, acetone was added twice to the precipitated mucilage to remove chlorophyll *via* centrifugation and repeated shaking (2500 rpm for 15 minutes). Subsequently, the precipitate mucilage was dried at 40 °C for 2 h and triturated to obtain a fine powder. Then, it was passed through sieve #100, and the final product was kept in a desiccator for further study.

2.2.2 Characterization of JLP

2.2.2.1 Phytoconstituent screening. Various phytoconstituents present in the extracted JLP were identified by different identification tests, such as Mayer's test, Fehling's test, Salkowski's test, Borntrager's tests, ferric chloride test, and Millon's test for alkaloids, carbohydrates, phytosterols, glycosides, tannins, amino acids, mucilage and starch. For carbohydrates, their presence was checked through Fehling's test by mixing drops of Fehling's A and B reagents and heating them in a water bath. For mucilage, to check the presence of mucilage in the sample, the Ruthenium red test was performed by observing stained dry JLP powder under a microscope. For the alkaloids, Dragendorff's test was performed to identify the presence of the alkaloids. 0.2 g of JLP was heated with methanol, filtered, acidified with HCl, and then treated with Dragendorff's reagent. In Mayer's test, 2 mL of concentrated HCl was added to 2 mL of 1% w/v JLP, followed by the addition of Mayer's reagent (2 drops). The Borntrager's test was performed for glycosides by adding 0.001 g of JLP powder to 2 mL of benzene; the solution was filtered, and 2.5 mL of 10% ammonia solution was added to the filtrate. In Legal's test 1% w/v JLP solution was treated with 2 mL pyridine and 2 mL sodium nitroprusside, followed by NaOH to make it alkaline. For starch, its presence was tested using an iodine test with 0.1 g of JLP and an iodine solution. For tannins, JLP was tested for the presence of tannins by adding lead acetate and ferric chloride to the JLP solutions. For proteins and amino acids, they were tested using the Ninhydrin test by adding 5 drops of 2% ninhydrin solution in acetone, which was added to 2 mL of 1% JLP and heated at 50 °C for 5 min. For steroids: the presence of steroids was checked through Libermann–Burchard's

 © 2026 The Author(s). Published by the Royal Society of Chemistry

Open Access Article. Published on 12 January 2026. Downloaded on 3/17/2026 6:44:35 PM.
This article is licensed under a Creative Commons Attribution-NonCommercial 3.0 Unported Licence.

test, involving the addition of 0.5 mL of acetic anhydride and 3 drops of concentrated sulfuric acid to 2.5 mL of 1% JLP solution.[19–21]

2.2.2.2 Organoleptic properties. The colour, odour, and taste of the JLP were observed manually.[22]

2.2.2.3 Total polysaccharide content. The total polysaccharide content in the extracted JLP was evaluated *via* spectrophotometric analysis. Glucose was used as the standard, and a standard curve was established using varying glucose concentrations (50 μg mL^{-1}, 60 μg mL^{-1}, 70 μg mL^{-1}, 80 μg mL^{-1}, 90 μg mL^{-1}, and 100 μg mL^{-1}). A 100 μg mL^{-1} aqueous solution of JLP was produced, from which 1 mL was extracted, to which 1 mL of 5% w/v phenol was added, followed by the addition of 5 mL of concentrated H_2SO_4. The resulting mixture was put aside for 10 minutes and subsequently analysed spectrophotometrically at 488 nm using a UV-visible spectrophotometer (UV-1900i, Shimadzu, Japan), relative to a blank subjected to identical treatment without JLP. The test was carried out in triplicate, and the mean value was obtained.[23]

2.2.2.4 ^{13}C solid-state NMR spectroscopy analysis. The solid-state NMR spectrum (^{13}C) of JLP was acquired using a Jeol Solid State NMR Spectrometer (Jeol Resonance, 400 MHz, Jeol, Japan) operating at 400 MHz with a 4 mm MAS probe.[24]

2.2.2.5 Elemental analysis. Carbon, hydrogen, sulphur, and nitrogen percentages of the JLP were determined with an elemental analyser (vario EL cube). A combustion temperature of 1050 °C was maintained, and helium was employed as a carrier.[25]

2.2.2.6 FTIR study. FTIR spectra of native JLP, DS and tablet were obtained from FTIR (Bruker, alpha II, ECO-ATR, Bruker, Germany) in order to analyse drug–excipient incompatibilities. A KBr pellet with a very small amount of each sample was scanned, ranging from 500 cm^{-1} to 4000 cm^{-1}.[18]

2.2.2.7 Molar mass, zeta potential and particle size. The molar mass, zeta potential, and particle size were determined using the Dynamic Light Scattering method with Litesizer 500, Anton Paar, Austria. In order to determine the molar mass of JLP, three aqueous solutions with concentrations of 0.01%, 0.02%, and 0.05% w/v were prepared. In the study, water with a refractive index of 1.3303 and dn/dc 1.0 mL g^{-1} was used as a solvent. Toluene with a refractive index of 1.4925 and a Rayleigh ratio of 0.0000115 cm^{-1} was used as a reference. The temperature was set at 25 °C. To determine zeta potential, water having a refractive index of 1.3303, viscosity of 0.0008903 Pa s, and relative permittivity of 78.37 was used as solvent, and the adjusted voltage, filter optical density, and temperature were 200.0 V, 2.0105, and 25.0 °C, respectively. For particle size, a freshly prepared 1% w/v aqueous suspension of JLP powder was used.[26]

2.2.2.8 Determination of aqueous solubility, pH, surface tension and viscosity. The aqueous solubility of JLP (1% w/v) was measured by preparing five distinct dispersions (1%, 2%, 3%, 4%, and 5% w/v) with magnetic stirring for 6 h continuously at 25 °C and continuous visual monitoring. The pH of the solution was assessed with a digital pH meter (pH 700, Eutech Instrument, Singapore) at 28.4 °C. The surface tension of a 1% w/v JLP solution was measured using a K9 optical tensiometer (Kruss GmbH, Hamburg, Germany). The viscosity of a 1% w/v JLP solution was measured using a Brookfield viscometer (LV, Ametek, USA) with spindle no. 64. The spindle was configured to run at 60 rpm and 30.6 °C.[27]

2.2.2.9 Swelling index. The swelling index (SI) of JLP was calculated following the method advised by the World Health Organization (WHO).[28] First, 25 mL of distilled water was filled in a glass-stoppered measuring cylinder. Subsequently, 1 g of JLP powder (previously sieved through sieve no. 120) was added to portions under continuous stirring to achieve uniform dispersion. Once the whole amount of powder was added, the mixture was mixed well at 10-minute intervals for 60 minutes. The volume occupied by the swollen mass at this time was noted.[29] This test was run in triplicate, and the swelling index was obtained using the following formula:

$$\text{Swelling index}\,(\%) = \frac{V_f - V_0}{V_0} \times 100,$$

where V_0 and V_f were the initial volume of dry powder and the final volume of hydrated swollen mass, respectively.

2.2.2.10 Determination of loss of drying. The moisture content and loss on drying (LOD) of the dried JLP powder were determined by employing the oven-drying technique. 1.00 g of JLP powdered sample was placed in a pre-weighed, dry watch glass (W_1), and the initial weight of the watch glass with the sample (W_2) was recorded. Moisture content was determined as a percentage of weight loss from the initial weight.[30,31] The sample was subjected to heating in a hot air oven at 105 ± 2 °C for 1 h, subsequently cooled to ambient temperature in a desiccator (25 ± 2 °C), and then reweighed (W_3). The process was continued until the difference between the two consecutive weights was less than 5 mg, indicating that a constant mass had been attained. The LOD was determined as the percentage of JLP powder weight loss after drying compared to the initial powder weight:[32]

$$\text{Loss on drying}\,(\%) = \frac{W_2 - W_3}{W_2 - W_1} \times 100.$$

2.2.2.11 Stability profile of JLP in an aqueous environment. The stability of JLP in the solution phase was evaluated using the UV–Visible spectroscopic method. 0.5% w/v JLP solution was prepared using a magnetic stirrer. The samples were withdrawn at different time intervals (at time 0 h, 12 h, 24 h, 48 h, 72 h, 120 h, 168 h) and analysed using a UV-visible spectrophotometer in the range of 200–600 nm.[33]

2.2.2.12 DSC, TGA and DTA study. Differential Scanning Calorimetry was determined for the extracted JLP using a Differential Scanning Calorimeter (Mettler Toledo, USA) at a heating rate of 10 °C min^{-1}. The sample was placed on a platinum crucible and heated at a rate of 150 mL min^{-1} of nitrogen between 30 °C and 400 °C. For this study, alpha alumina powder served as a reference. To obtain DTA and TGA thermograms, a thermogravimetric analyser (DTG-60, Shimadzu, Japan) was used.[34]

Open Access Article. Published on 12 January 2026. Downloaded on 3/17/2026 6:44:35 PM.
This article is licensed under a Creative Commons Attribution-NonCommercial 3.0 Unported Licence.

2.2.2.13 Powder XRD study. Powder X-ray diffraction patterns (PXRD) of native JLP, drug and tablet were obtained at 25 °C using an XRD diffractometer (Smart Lab 9 kW, Rigaku, Japan) with nickel filtered CuK alpha 1 radiation (1.54060 Å) at a 40 kV voltage and 30 mA current. The range of the scattering angle (2θ) was 0–90°with a minimum step size of 0.001°.[35]

2.2.2.14 Scanning electron microscopy (SEM). The surface topography of the extracted JLP was observed using an SEM (Mettler Toledo, USA) study. The surface topography of the compressed tablet and the dried tablet collected in the middle of the release study was also studied. The samples were kept on both sides of adhesive tape, which was kept under vacuum and subjected to gold coating to increase conductivity. A working distance of 7 mm was maintained with an applied voltage of 2.0 kV.[36]

2.2.3 Preformulation studies. Various preformulation tests were conducted to examine the compatibility of pure DS and other excipients using FTIR, TGA, DTA, and DSC, as previously described. The crystallinity of the pure DS and tablet matrices was assessed by PXRD analysis.

2.2.4 Preparation and evaluation of DS matrix tablets

2.2.4.1 Preparation of DS tablets using the wet granulation technique. Matrix tablets containing DS were developed using the wet granulation method. As shown in Table 1, native JLP, starch, and PVP K-30 were used individually for various formulation batches. The drug was accurately weighed and mixed homogeneously with the polymer. The drug–polymer mixture was mixed thoroughly with half the amount of talc and magnesium stearate. A certain amount of lactose was added as a tablet diluent. Distilled water was used with the drug–excipient mixture to prepare a moist mass. The wet mass was passed through sieve no. 12. The prepared granules were placed in a hot-air oven (Indian Instruments Manufacturing Co.) at 50 °C for drying. The remaining magnesium stearate and talc were added to the dried granules and screened through sieve no. 18 to achieve a uniform granule size. The tablets were prepared using a rotary tablet compression machine (Kambert Machinery, India) with a 6 mm die.[8]

2.2.4.2 Derived and micromeritic properties of granules. The granule size distribution was investigated through sieve analysis by employing a standard sieve set. The bulk volume of particles can be determined using a graduated measuring cylinder. A specified quantity of granules was placed into a 100 mL graduated cylinder, and the volume they occupied was recorded as bulk volume. The bulk density of the granules was obtained using the bulk volume and the precise weight of the granules evaluated in the study.[37] The bulk density was calculated using the following equation:

$$\text{Bulk density granules} = \frac{\text{mass of granules taken}}{\text{bulk volume of granules}}.$$

The tapped density of the granules was obtained by measuring the tapped volume (V_t) once a constant volume was achieved using a tapped density device (Model TD-1025, LabIndia, India). Granules were weighed, transferred into a graduated cylinder and tapped within the device. The ultimate settling volume was recorded after tapping continued until no more volume change was seen.[37] The tapped density was calculated using the following equation:

$$\text{Tapped density of granules} = \frac{\text{mass of granules taken}}{\text{tapped volume of granules}}.$$

The Carr's compressibility index was calculated using the following formula:

$$\text{Carr's index} = \frac{\text{tapped density} - \text{bulk density}}{\text{tapped density}} \times 100\%.$$

Hausner's ratio was determined using the following equation:

$$\text{Hausner's ratio} = \frac{\text{tapped density of granules}}{\text{bulk density of granules}}.$$

The prepared granules were assessed for their flow characteristics by determining the angle of repose. The angle of repose was obtained using the fixed funnel method. This approach required securing a funnel with its tip positioned at a specified height (h) above graph paper placed on a level horizontal base. The granules were precisely poured into the funnel until the peak of the conical heap barely contacted the tip of the funnel. The radius of the base of the conical pile was measured. The radius (r) of the heap was measured by recording the diameter of the circular base and taking half of this value.[27,38] The

Table 1 Composition of various DS incorporated tablet batches with varying concentrations of JLP, starch, and PVP K-30

Batch no.	Drug (diclofenac sodium)	JLP	Starch	PVP K-30	Lactose	Talc	Mg stearate
B1	50 mg	2.5%	—	—	135 mg	5 mg	5 mg
B2	50 mg	5%	—	—	130 mg	5 mg	5 mg
B3	50 mg	7.5%	—	—	125 mg	5 mg	5 mg
B4	50 mg	10%	—	—	120 mg	5 mg	5 mg
B5	50 mg	—	2.5%	—	135 mg	5 mg	5 mg
B6	50 mg	—	5%	—	130 mg	5 mg	5 mg
B7	50 mg	—	7.5%	—	125 mg	5 mg	5 mg
B8	50 mg	—	10%	—	120 mg	5 mg	5 mg
B9	50 mg	—	—	2.5%	135 mg	5 mg	5 mg
B10	50 mg	—	—	5%	130 mg	5 mg	5 mg
B11	50 mg	—	—	7.5%	125 mg	5 mg	5 mg
B12	50 mg	—	—	10%	120 mg	5 mg	5 mg

 © 2026 The Author(s). Published by the Royal Society of Chemistry

Open Access Article. Published on 12 January 2026. Downloaded on 3/17/2026 6:44:35 PM.
This article is licensed under a Creative Commons Attribution-NonCommercial 3.0 Unported Licence.

flow properties of the granules were evaluated by determining the angle of repose using the following formula:

$$\text{Angle of repose } (\theta) = \frac{\text{height of the heap}}{\text{radius of the heap}}.$$

2.2.4.3 Evaluation of DS matrix tablets

2.2.4.3.1Content uniformity. Ten tablets were randomly selected and weighed separately from each prepared batch of DS matrix tablets.[39] The tablets were subsequently ground into fine powder, and a precisely measured equivalent amount of 50 mg of DS was placed into a 100 mL volumetric flask. Distilled water was introduced, and the flask was placed on a mechanical shaker for 15 minutes. After passing the content *via* Whatman filter paper, the first 15 mL was allowed to be thrown away. After precisely measuring 10 millilitres of filtrate solution, 100 millilitres of solution were prepared by diluting it with distilled water. From the resulting solution, 10 mL was taken and diluted to 100 mL using distilled water. The drug content of the resultant solution was determined using a UV–Vis spectrophotometer (UV-1900i, Shimadzu) at 275 nm.

2.2.4.3.2Weight variation

Randomly, 20 tablets from each batch of DS matrix tablets were individually weighed using an electronic balance (Mettler, Toledo). The percentage relative standard deviation was determined from the obtained results.[40]

2.2.4.3.3Tablet hardness

A tablet hardness test was performed on five randomly chosen tablets using the Monsanto tablet hardness tester. The mean hardness was also recorded.[41]

2.2.4.3.4Percentage friability

Percentage friability was performed using a Roche tablet friability testing device (EF-2L, Friability Tester, Electrolab, India). Ten tablets were randomly selected from each formulation batch and collectively weighed to obtain the initial weight (W_0). These tablets were then placed in the chamber of a friability test apparatus, which was allowed to rotate at 25 revolutions per minute (rpm) for a total of 100 rotations.[42] After completion, the tablets were collected, cleaned to eliminate any loose particles, and reweighed to ascertain the final weight (W_f). The following formula can be used to determine percentage friability:

$$\text{Percentage friability} = \frac{W_0 - W_f}{W_0} \times 100.$$

2.2.4.3.5Disintegration time

Six tablets were randomly chosen from each prepared batch and studied for disintegration using a tablet disintegration apparatus (Lab India, model-DT 1000). Using phosphate buffer (pH 7.5) as a disintegration medium, the temperature was kept at 37 °C ± 0.5 °C. The tablets were placed in the basket, and the time necessary for total disintegration was ascertained. The average disintegration time in minutes was determined for each formulation batch.[42]

2.2.4.3.6*In vitro* dissolution study

The prepared DS matrix tablets were assessed for *in vitro* dissolution using simulated intestinal fluid (phosphate buffer, pH 7.5). The study was conducted using a USP Class II dissolution test apparatus. The stirrer speed was kept at 50 rpm. The bath temperature was maintained at 37 ± 0.5 °C throughout the experiment. At predetermined intervals, 5 mL of dissolution solution was removed and replaced with the equivalent volume of freshly prepared buffer solution. The withdrawn sample was immediately filtered, and the amount of drug released was analysed spectrophotometrically (UV-1900i, Shimadzu) at λ_{max} of 275 nm. The cumulative percentage release (CPR) of the drugs was determined using the obtained values. After conducting the trial three times, the mean CPR value was determined.[43]

2.2.4.3.7Drug release kinetics

The average CPR values were aligned with many kinetic models, as detailed below. Zero-order kinetics: $Q_t = Q_0 + K_0 \cdot t$, where Q_t is the dissolved amount of drug after time t, Q_0 is the initial amount of drug in solution, and K_0 is the zero-order constant. First order kinetics: $\log Q_t = \log Q_0 + K_1 \cdot \frac{t}{2.303}$, K_1 is the first order constant. Higuchi kinetics: $Q = k_H \cdot t^{\left\{\frac{1}{2}\right\}}$, where Q is the dissolved amount of drug after time t and K_H is the Higuchi constant. Hixon–Crowell kinetics: $Q_{\{0\}}^{\left\{\frac{1}{3}\right\}} - Q_{\{t\}}^{\left\{\frac{1}{3}\right\}} = K_{\{HC\}} \cdot t$, where Q_0 is the dissolved amount of drug after time t, Q_t is the initial amount of drug in solution and K is the zero-order constant. Korsmeyer–Peppas kinetics: $Q = Kt^n$, where Q is the fraction of dissolved drug after time t, and K and n are the rate constant and diffusional exponent, respectively. Korsmeyer–Peppas kinetics was also employed to predict the drug release mechanism, including diffusion-controlled release (Fickian mechanism), anomalous transport (non-Fickian mechanism), and relaxation-controlled drug release (case-II transport) mechanism.[49] The n value of ≤0.43 indicates the Fickian release mechanism, a value in the range of 0.43–0.85 predicts non-Fickian release, and an n value of ≥0.85 indicates case-II transport.[43]

2.2.4.3.8Stability study

The JLP (batch B1) tablets were stored in a stability chamber for three months at 40 °C ± 0.5 °C and 75% ± 5% relative humidity in an airtight, clean glass container. After three months, the aged tablets were examined for variations in appearance and assessed for drug content, hardness, *in vitro* dissolution, and FTIR.[44]

2.2.5 Statistical analysis. MedCalc software (11.6.1.0. version) was used to perform a basic statistical analysis of the information obtained.

3. Results and discussion

3.1 Characterizations of JLP

3.1.1 Phytoconstituent screening. The presence of carbohydrates and mucilage in extracted JLP was investigated by phytochemical screening (Table 2). Dragendroff's and Mayer's reagents used to study the alkaloid content demonstrated the absence of alkaloids in JLP. Comprehensive testing involving Borntrager's, Keller–Kiliani, Legal's, iodine, lead acetate, ferric chloride, Ninhydrin, and Libermann–Burchard's tests indi-

Open Access Article. Published on 12 January 2026. Downloaded on 3/17/2026 6:44:35 PM.
This article is licensed under a Creative Commons Attribution-NonCommercial 3.0 Unported Licence.

Table 2 Phytochemical evaluations of the extracted JLP

Sl. no.	Performed tests	Name of tests	Inference
1	Carbohydrate test	Fehling's test	Positive
2	Mucilage test	Ruthenium red test	Positive
3	Starch test	Iodine test	Negative
4	Alkaloid test	Dragendroff's test & Mayer's test	Negative
5	Glycoside test	Legal test and Borntrager test	Negative
6	Test for tannins	Ferric chloride and lead acetate test	Negative
7	Steroids and sterols	Libermann–Burchard's test	Negative
8	Proteins and amino acids test	Ninhydrin test	Negative

cated the absence of glycosides, starch, tannins, proteins, amino acids, or steroidal substances.[45]

3.1.2 Total polysaccharide content. The JLP sample comprised 74.17% ± 0.031% w/w total polysaccharides, as determined by UV-visible spectroscopy at 484 nm. A similar type of glucose calibration curve (50–100 μg mL^{-1}) with high linearity (r^2 = 0.995) was observed by Guo *et al.* and extracted from the seeds of *Sophora alopecuroides* L. (78.4% w/w).[46]

3.1.3 ^{13}C solid-state NMR spectroscopy analysis. The solid-state ^{13}C NMR spectra of jute leaf polysaccharide (JLP) (S1) displayed multiple distinctive resonances that confirmed its polysaccharide backbone and functional group substituents, as shown in Fig. 1. A significant resonance at 99.658 ppm was attributed to the anomeric carbon (C1) of the sugar residues, while the pronounced signal at 72.911 ppm was associated with the ring carbons (C2, C3, and C5) of the pyranose units. The resonance at 53.939 ppm was ascribed to C–N modified carbons or methoxy carbons linked to acetylated or amine-containing polysaccharides. Signals detected at 37.019, 33.003, and 30.695 ppm corresponded to aliphatic methylene carbons ($-CH_2-$), while those at 21.894 and 18.39 ppm signified methyl carbons ($-CH_3$), presumably originating from acetyl substituents. A characteristic downward resonance at 175.372 ppm indicated carbonyl carbons (C═O) either from uronic acid residues or ester/amide linkages, hence affirming the polysaccharide composition of JLP with potential acetyl and uronic replacements.[23]

3.1.4 Elemental analysis. The elemental analysis of extracted JLP revealed the presence of carbon, hydrogen, nitrogen, and sulphur, with contents of 33.68%, 5.677%, 1.98%, and 0.161%, respectively. This result was found to be similar to the elemental contents of JLP reported by Wang *et al.* and Tang *et al.*[47,48]

3.1.5 FTIR analysis. The FTIR spectra of the pure DS, JLP, and tablet formulations are illustrated in Fig. 2. The JLP spectrum exhibits extensive absorption characteristics of polysaccharides, featuring a large O–H stretching band at 3239.36 cm^{-1}, C–H stretching vibrations throughout the 2920–2850 cm^{-1} range, and pronounced C–O/C–O–C bands in

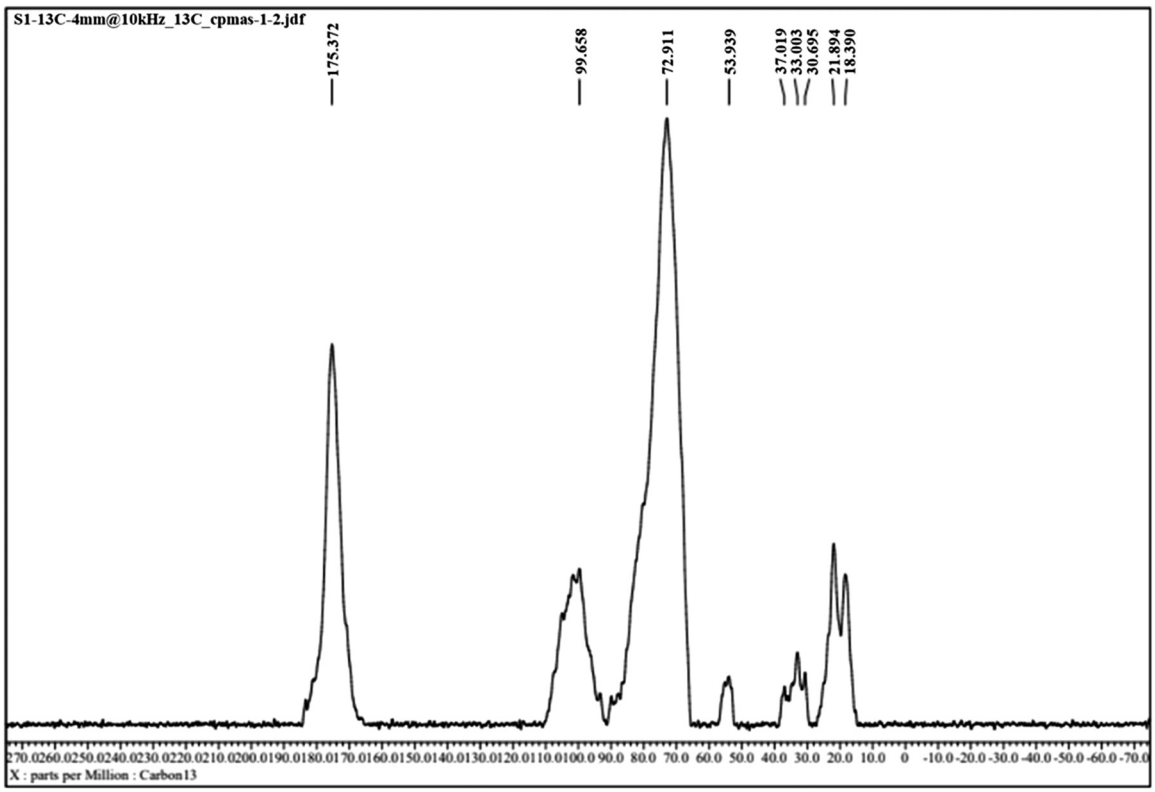

Fig. 1 NMR spectrum of JLP.

 © 2026 The Author(s). Published by the Royal Society of Chemistry

Open Access Article. Published on 12 January 2026. Downloaded on 3/17/2026 6:44:35 PM.
This article is licensed under a Creative Commons Attribution-NonCommercial 3.0 Unported Licence.

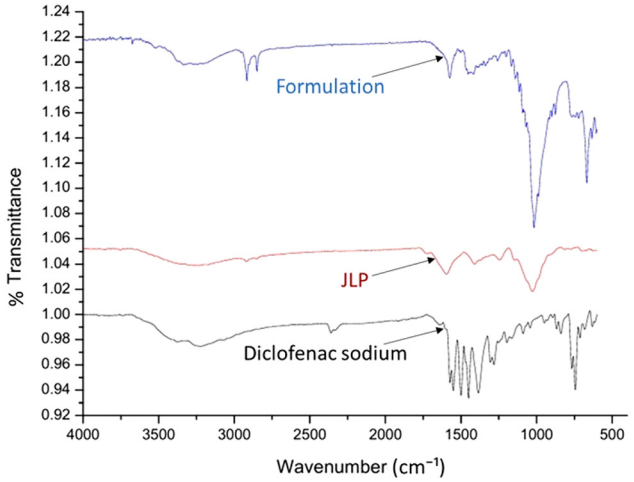

Fig. 2 FTIR spectra of native JLP, pure DS, and DS-loaded tablet (B1 batch).

the 1200–1000 cm^{-1} region. Pure DS exhibits characteristic drug absorptions, including a large N–H/O–H related band about 3370 cm^{-1}, aromatic C–H stretches approximately at 3000 cm^{-1}, and pronounced bands associated with the carboxylate/carboxyl functionality (C═O/C–O stretching) at around 1574 cm^{-1}. The FTIR spectrum of the tablet formulation contained the primary DS peaks—the N–H/O–H band (~3370 cm^{-1}), the carboxylate C═O/C–O band (~1574–1575 cm^{-1}), the aromatic C–C in-ring band (~1452 cm^{-1}), and the C–N stretching near 1305 cm^{-1}—without significant shifts or loss of these distinctive signals. The persistence of the drug's characteristic absorptions in the formulation spectrum signifies the presence of DS in the tablet and implies the absence of major chemical interactions (*e.g.*, bond formation or degradation) between DS and the JLP excipient under the preparation conditions employed. The tablet spectrum shows both sets of analytical groups (JLP and diclofenac) without significant changes or drug spectrum disappearance, indicating physicochemical stability in the formulation.[18]

3.1.6 Molar mass, zeta potential, and particle size. The molar mass, zeta potential, average particle size, and polydispersity index are displayed in Table 3. The molar mass of extracted JLP was found to be 2.12 (±0.05) × 10^5 Da, which is relatively higher than the molar mass of TSP derived from the taro (*Colocasia esculenta*) stolon polysaccharide.[49] The mean zeta potential was found to be −4.6 (±0.4) mV. The negative zeta potential may have resulted from the presence of –COOH groups. The average particle size was found to be 438.6 nm.

3.1.7 Determination of pH, surface tension, viscosity, and water solubility. The pH, surface tension, and viscosity of the 1% w/v aqueous solution of JLP were found to be 6.88 ± 0.03, 76.73 ± 0.06 dyne cm^{-1}, and 900.04 ± 0.01 cP, respectively (as shown in Table 3). A pH of 6.88 ± 0.03 signifies that the JLP solution is nearly neutral, which suggests that it may be biocompatible and appropriate for topical and oral use. Because of this neutral pH, there is less chance that pH-sensitive active substances will become irritated or degrade. The surface tension of 76.73 ± 0.06 dyne cm^{-1}, although slightly less than that of pure water (~72.8 dyne cm^{-1}), indicates a moderate wetting ability, perhaps enhancing spreading over drug particles during wet granulation and promoting uniform binder dispersion. The high viscosity of 900.04 ± 0.01 cP indicates effective thickening and binding capabilities.[26] In the solubility study, JLP was observed to be dissolved and yielded a clear and transparent aqueous dispersion up to 2% w/v concentration.

Table 3 Physicochemical characteristics of JLP

Physicochemical characteristics	Values
Color	Greyish brown
Odor	Odourless
Taste	Bland
Polysaccharide content	74.17 ± 0.031
Elements present	N [1.98%], C [33.68%], H [5,677%], S [0.161%]
Molar mass	2.12 (±0.05) × 10^5 Da
Zeta potential	−4.6 (±0.4) mV
Viscosity (1% w/v)	900.04 ± 0.01 Cp
pH (1% w/v)	6.88 ± 0.021
Aqueous solubility	Soluble up to 2% w/v
Surface tension (1% w/v)	76.73 ± 0.06 dyne cm^{-1}
Particle size	438.6 nm
Swelling index	1113.4% ± 4.77% ml g^{-1}
Loss on drying	9.86% ± 0.15% w/w

3.1.8 Swelling index. The swelling index of the JLP samples was assessed using distilled water as a medium, as described by the WHO for evaluating the swelling index of crude drugs, demonstrating the superior swelling characteristics of the JLP. After 4 h, the swelling index was observed to be 1113.40% ± 4.77% with regard to the volume occupied by 1 g of dry powder. A considerable increase in the swelling index was observed over time. The increased swelling index further indicates the efficiency of JLP as a disintegrating agent for matrix tablets.[50]

3.1.9 Determination of loss on drying. The percentage moisture content of the JLP powder expressed as a percentage loss on drying (LOD) was found to be 9.86% ± 0.15% w/w, indicating the mass lost during heating at 105 °C. The loss of moisture is predominantly caused by free and bound water inside the polysaccharide structure.[32]

3.1.10 Stability profile of JLP in an aqueous environment. UV–visible spectral analysis showed a significant decrease in absorbance over time, signifying the continuous degradation of JLP. All the JLP samples at different time intervals are analyzed between the wavelengths 200 and 600 nm, as depicted in Fig. 3. The spectral representation exhibited considerable change from 24 h to 48 h data and from 48 h to 72 h data. This indicates the occurrence of probable bacterial growth during this time. The visual appearance and smell of the product were also noticed during this time. The absorbance against the wavelength (nm) measured at various time intervals is represented by each curve. Since JLP is obtained from a natural source, the change may be attributable to microbial proliferation or biochemical degradation.[33]

Open Access Article. Published on 12 January 2026. Downloaded on 3/17/2026 6:44:35 PM.
This article is licensed under a Creative Commons Attribution-NonCommercial 3.0 Unported Licence.

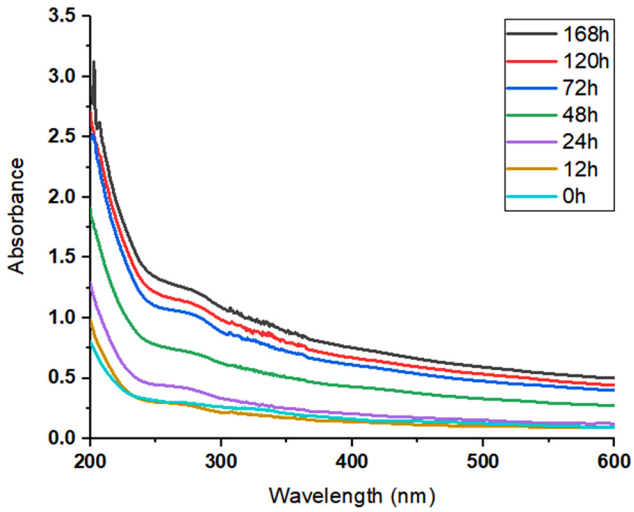

Fig. 3 Stability assessment of JLP in aqueous environment.

3.1.11 DSC, TGA, and DTA. The DSC thermograms of the JLP, pure DS, and prepared diclofenac tablets are displayed in Fig. 4. The thermogram exhibited two distinct endothermic peaks. The JLP thermogram showed that an endothermic peak was observed at 77.65 °C, which may correspond to the evaporation of moisture (free or bound water) or other volatile components present in the sample. A second sharp endothermic peak was observed at 312.83 °C, which can be attributed to the melting of the crystalline drug (DS) or thermal degradation of the polymer matrix. The absence of any additional endothermic or exothermic peaks suggests no major polymorphic transition or chemical incompatibility under the studied conditions. The thermogram for DS displayed an endothermic peak of around 75.74 °C, which indicates the loss of water (dehydration) from the hydrated DS salt. A similar endothermic peak in the thermogram of pure DS was also reported by Manna *et al.*[8] The second, more prominent, sharp endothermic peak was observed at approximately 287.08 °C, and a subsequent exothermic peak was observed at 294.73 °C. The sharp endothermic peak signifies the melting point of the anhydrous DS, while the subsequent exothermic peak is likely due to the decomposition of the drug. The Differential Scanning Calorimetry (DSC) thermogram for the JLP tablet exhibits three significant thermal peaks. A broad endothermic peak at approximately 64.40 °C suggests the loss of moisture or the melting of a low-temperature excipient. The subsequent endothermic peaks at 256.14 °C and 279.34 °C likely correspond to the melting of the active pharmaceutical ingredient and another component or a polymorphic transition, respectively, followed by potential decomposition.

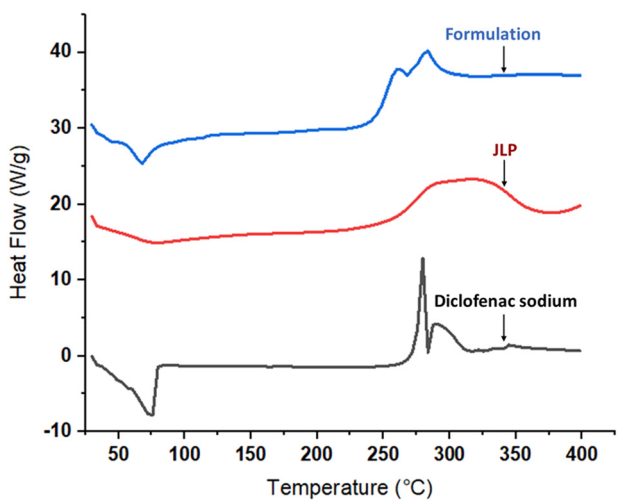

Fig. 4 DSC thermograms of native JLP, pure DS, and tablet formulation (B1 batch).

The TGA thermogram of JLP shows a weight loss of 9.77% between 25 °C and 105 °C, which is likely due to the loss of moisture. A further weight loss of 25.43% occurs between 105 °C and 400 °C, and a third weight loss of 28.51% is observed between 400 °C and 600 °C. These two later stages of weight loss are associated with the thermal degradation of the JLP. The DTA thermogram of JLP exhibits endothermic peaks at 77.29 °C and 278.44 °C, along with an exothermic peak at 494.39 °C. These peaks correspond to the dehydration and degradation processes observed in the TGA analysis. The TGA thermogram for DS shows an initial weight loss of 0.81% from 25 °C to 110 °C, which is attributed to moisture loss. A second, more significant weight loss of 30.68% is observed between 290 °C and 400 °C, followed by another weight loss of 19.33% between 400 °C and 500 °C. These weight losses are due to the degradation of the DS molecule. The DTA thermogram for DS shows two endothermic peaks: a small one at 122.95 °C and a sharp one at 292.05 °C. The sharp peak at 292.05 °C corresponds to the melting point of the DS. The TGA thermogram of the JLP tablet shows a weight loss of 2.19% from 25 °C to 120 °C, which corresponds to the loss of moisture. A second major weight loss of 29.58% is observed between 280 °C and 400 °C. This is followed by a third weight loss of 19.12% between 400 °C and 600 °C. These two stages of weight loss are attributed to the degradation of the tablet's components, including DS and the JLP plant material. The DTA thermogram of the JLP tablet displays endothermic peaks at 82.26 °C and 290.49 °C, and an exothermic peak at 485.49 °C. The peak at 290.49 °C indicates the melting point of DS, while the other peaks are associated with the degradation of the other tablet excipients and the JLP.[8]

3.1.12 Powder X-ray diffraction. A PXRD study was performed for JLP, pure DS, and DS-containing tablet (B1 batch) formulations. The obtained diffractograms are depicted in Fig. 5. The JLP diffractogram showed a broad halo-like pattern with low-intensity peaks, particularly in the range of ~10°–30° (2θ), and an absence of sharp high-intensity peaks. The X-ray diffraction pattern of DS exhibits numerous sharp and intense peaks, particularly in the 2θ range of approximately 10°–30°, with the highest intensity exceeding 500 counts. The presence of these well-defined diffraction peaks confirms the highly

 © 2026 The Author(s). Published by the Royal Society of Chemistry

Open Access Article. Published on 12 January 2026. Downloaded on 3/17/2026 6:44:35 PM.
This article is licensed under a Creative Commons Attribution-NonCommercial 3.0 Unported Licence.

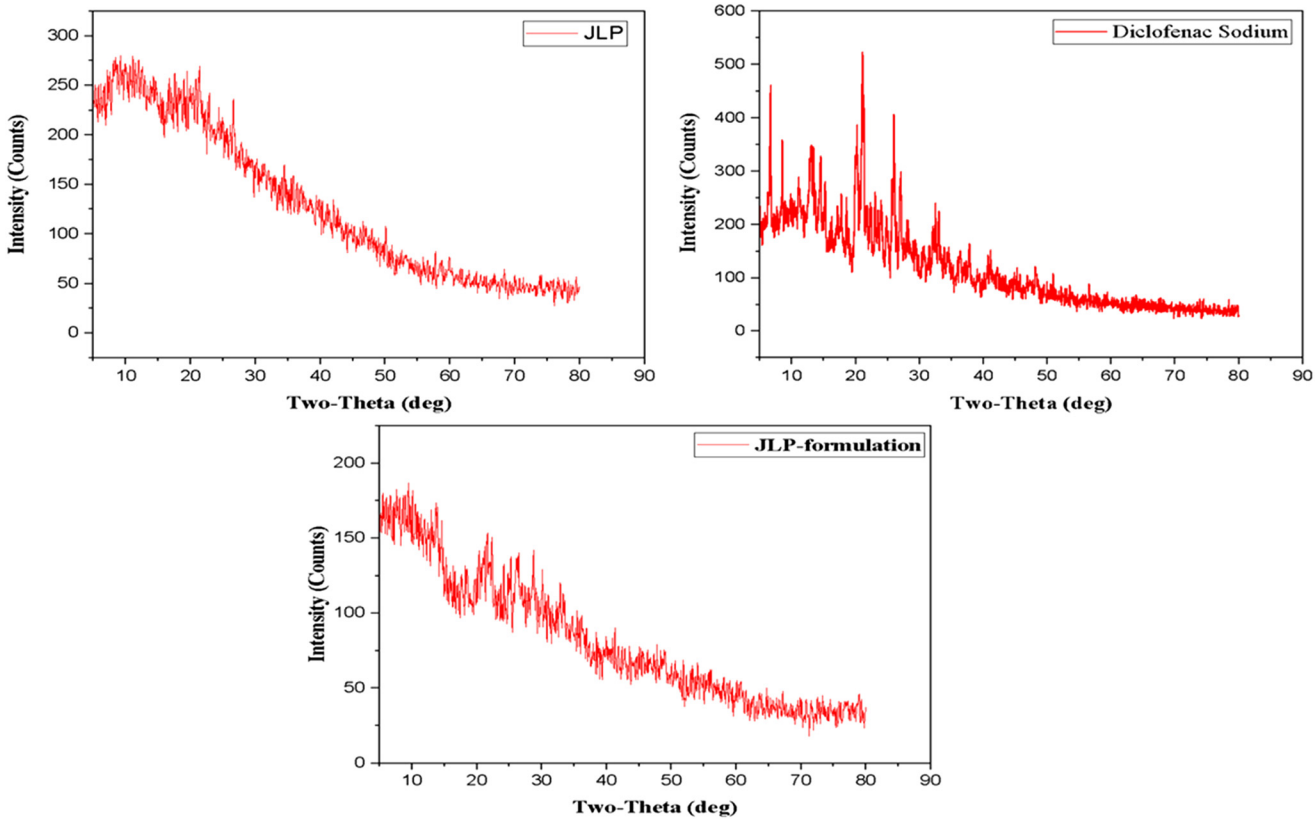

Fig. 5 Powder X-ray diffractograms of JLP, pure DS and tablet formulation (B1 batch).

crystalline nature of DS. The diffractogram displays a broad halo-like peak and a lack of sharp, intense diffraction peaks. This suggests that the jute leaf polysaccharide (JLP) formulation is primarily amorphous rather than crystalline. The intensity peaks in the low 2θ range (about 10°–20°) and progressively diminishes at higher angles (20°–80°). This pattern indicates amorphous polysaccharides.[35]

3.1.13 Scanning electron microscopy. The SEM image of the dried powdered JLP is depicted in Fig. 6. Fig. 6A reveals that the native JLP particles exhibit irregular morphology with a rough and crumpled surface. Surface roughness indicates a high surface area, which may improve interactions with solvents or active compounds. The higher magnification (Fig. 6B) shows fine granularity and possibly micro-flaws or layered structures. The SEM images of developed JLP-based tablets (Fig. 6C) depicted the dry, smooth and compact surface of a compressed tablet before dissolution. The micrograph showed minimal pores or cracks on the surface. The dried mid-dissolution tablet surface image (Fig. 6D) displayed an erodible and swollen surface with highly porous and roughness present on it. The comparison of the SEM results demonstrates that drug release from the tablet matrix is facilitated by surface erosion and pore development relies on dissolution. The transformation from a dense structure to a porous, degraded surface shows the efficacy of the disintegration and dissolution processes.[25]

3.2 Evaluation of the granules

The various derived and micromeritic properties of the developed granules are presented in Table 4. The granules exhibited a relatively uniform mean size, ranging from 1058.52 ± 11.04 μm to 1056.14 ± 17.82 μm, which is equivalent to the granule size of DS using jute leaf polysaccharides as binders. This was similar to the size of the granules of DS formulated using *Cassia fistula* seed galactomannan as a binder.[26] The bulk density of the developed granule batches ranged from 0.5357 g cm^{-3} to 0.5769 g cm^{-3}, which was very similar to the diclofenac incorporated granules prepared using *Cassia fistula* seed galactomannan.[26] The developed granules had measured tapped densities ranging from 0.6117 ± 0.0044 g cm^{-3} to 0.6534 ± 0.0047 g cm^{-3}, which were similar to paracetamol granules made with the mucilage from *Mimosa pudica* seeds as a binder.[51] Good flow behaviour was shown by the Carr's index, which ranged from 11.70 ± 0.0476 to 12.42 ± 0.0891 for all of the batches. Additionally, the Hausner's ratio varied between 1.133 ± 0.0006 and 1.142 ± 0.0012, indicating that the granules had good flow properties. Hausner's ratio and Carr's index values were similar to those of paracetamol granules developed with cashew tree gum and mimosa mucilage as a binder.[51] In accordance with earlier reports on paracetamol granules prepared with mimosa mucilage, the angle of repose values ranged from 23.558 ± 0.4028° to 28.641 ± 0.348°.[51] It

Open Access Article. Published on 12 January 2026. Downloaded on 3/17/2026 6:44:35 PM.
This article is licensed under a Creative Commons Attribution-NonCommercial 3.0 Unported Licence.

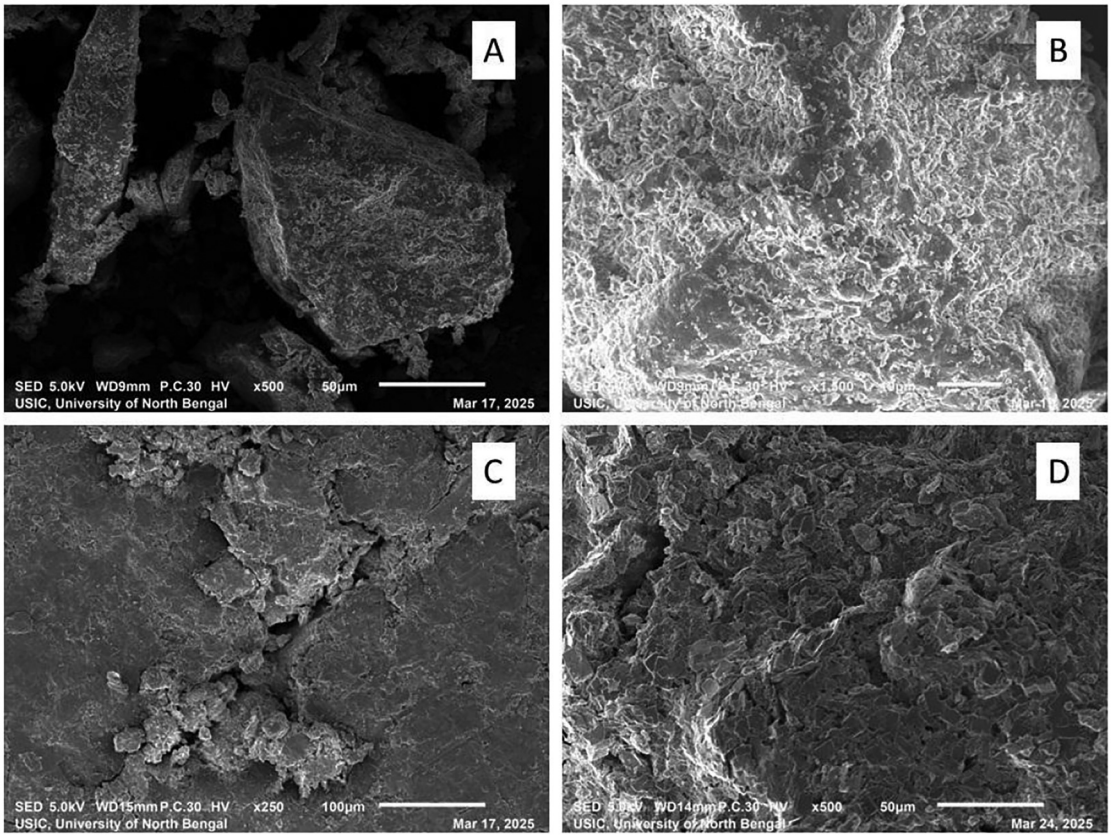

Fig. 6 SEM images of (A) dried JLP powder particles at 500× magnification; (B) JLP powder particles at higher magnification (1500×); (C) compressed tablet surface before dissolution; and (D) porous surface during tablet dissolution.

Table 4 Different derived micromeritic properties of various prepared granule batches

Batch no.	Size of granules (mean ± S.D.) (n = 3)	Bulk volume (cm^3) (mean ± S.D.) (n = 3)	Bulk density ($g\ cm^{-3}$) (mean ± S.D.) (n = 3)	Tapped density ($g\ cm^{-3}$) (mean ± S.D.) (n = 3)	Carr's index (mean ± S.D.) (n = 3)	Hausner's ratio (mean ± S.D.) (n = 3)	Angle of repose (°) (mean ± S.D.) (n = 3)
B1	1058.52 ± 1.04	18.67 ± 0.15	0.5357 ± 0.0044	0.6117 ± 0.0044	12.42 ± 0.0891	1.142 ± 0.0012	23.558 ± 0.4028
B2	1059.75 ± 6.62	18.83 ± 0.15	0.5310 ± 0.0043	0.6078 ± 0.0054	12.63 ± 0.135	1.145 ± 0.0018	25.296 ± 0.3812
B3	1057.5 ± 5.57	18.83 ± 0.208	0.5310 ± 0.0059	0.6075 ± 0.0067	12.59 ± 0.0296	1.144 ± 0.0004	27.49 ± 0.4106
B4	1064.78 ± 10.03	18.73 ± 0.208	0.5339 ± 0.006	0.6104 ± 0.0068	12.53 ± 0.0295	1.143 ± 0.0004	27.528 ± 0.3932
B5	1067.82 ± 3.7	17.3 ± 0.12	0.578 ± 0.0033	0.6545 ± 0.0026	11.69 ± 0.1712	1.132 ± 0.0022	26.46 ± 0.4623
B6	1064.96 ± 4.24	17.23 ± 0.06	0.5803 ± 0.0019	0.6568 ± 0.0025	11.65 ± 0.1034	1.132 ± 0.0013	26.531 ± 0.4034
B7	1059.77 ± 2.06	17.27 ± 0.12	0.5792 ± 0.0039	0.6552 ± 0.0038	11.60 ± 0.0685	1.131 ± 0.0009	28.576 ± 0.3928
B8	1050.5 ± 4.33	17.3 ± 0.1	0.578 ± 0.0033	0.6548 ± 0.0045	11.72 ± 0.13	1.133 ± 0.0017	26.565 ± 0.4884
B9	1058.62 ± 6.7	17.33 ± 0.06	0.5769 ± 0.0019	0.6534 ± 0.0025	11.70 ± 0.1039	1.133 ± 0.0013	25.637 ± 0.4355
B10	1058.12 ± 4.54	17.27 ± 0.12	0.5792 ± 0.0039	0.6552 ± 0.0039	11.60 ± 0.0685	1.131 ± 0.0009	26.54 ± 0.4034
B11	1051.08 ± 6.53	17.27 ± 0.06	0.5792 ± 0.0019	0.6559 ± 0.0017	11.70 ± 0.1981	1.133 ± 0.0025	27.5 ± 0.3827
B12	1056.14 ± 17.82	17.33 ± 0.12	0.5769 ± 0.0038	0.6534 ± 0.0047	11.70 ± 0.0476	1.133 ± 0.0006	28.641 ± 0.348

was discovered that the angle of repose increased as the polymer concentration increased. The results revealed that the developed granules had good flowability.

3.3 Evaluation of the prepared tablets

3.3.1 General evaluation parameters of tablets. Various evaluation parameters for prepared tablet batches are depicted in Table 5. The content uniformity of the developed tablet formulations was found to be between 99.43 ± 0.373 and 98.377% ± 0.286%. The almost similar drug contents of the formulations demonstrated the uniformity of the manufactured tablet batches. 20 tablets were selected at random from each batch to conduct a weight variation test. For each formulation, the average tablet weight was found to be within the Pharmacopoeial limits. The range of the average hardness was 4.22 ± 0.105 to 4.66 ± 0.085. A gradual rise in the concentration

 © 2026 The Author(s). Published by the Royal Society of Chemistry

Open Access Article. Published on 12 January 2026. Downloaded on 3/17/2026 6:44:35 PM.
This article is licensed under a Creative Commons Attribution-NonCommercial 3.0 Unported Licence.

Table 5 Post-compression characteristics of tablets from various batches

Batch no.	Content uniformity ± S.D. (%) (n = 10)	Tablet hardness ± S.D. (kg m^{-2}) (n = 5)	Percentage friability ± S.D. (n = 10)	Disintegration time ± S.D. (min) (n = 6)
B1	99.43 ± 0.373	4.22 ± 0.105	0.308 ± 0.057	8.28 ± 0.360
B2	99.63 ± 0.525	4.36 ± 0.117	0.265 ± 0.043	9.33 ± 0.534
B3	98.64 ± 0.532	4.46 ± 0.115	0.246 ± 0.046	11.62 ± 0.469
B4	98.62 ± 0.465	4.78 ± 0.078	0.241 ± 0.043	13.67 ± 0.44
B5	98.54 ± 0.346	4.09 ± 0.083	0.213 ± 0.015	5.31 ± 0.19
B6	98.47 ± 0.352	4.25 ± 0.156	0.230 ± 0.036	6.61 ± 0.373
B7	98.49 ± 0.425	4.38 ± 0.1	0.225 ± 0.038	7.51 ± 0.417
B8	98.4 ± 0.425	4.51 ± 0.141	0.279 ± 0.041	9.18 ± 0.512
B9	99.55 ± 0.142	4.07 ± 0.084	0.352 ± 0.045	7.31 ± 0.217
B10	99.36 ± 0.479	4.27 ± 0.085	0.263 ± 0.052	7.47 ± 0.421
B11	98.47 ± 0.355	4.52 ± 0.095	0.339 ± 0.046	7.61 ± 0.335
B12	98.377 ± 0.286	4.66 ± 0.085	0.238 ± 0.050	8.53 ± 0.246

of polymers was shown to increase hardness. According to Pharmacopoeial standards, the friability of prepared tablets was assessed and reported to be between 0.308 and 0.238%, which was below the permitted limit of friability (<1%). The obtained % friability shows outstanding physical stability for all developed formulations. The concentration of the binder significantly influenced the mechanical strength of the formulated tablets, as depicted in Fig. 7. Despite the increase in binder concentration, tablet hardness correspondingly increased, signifying enhanced inter particulate bonding. The increasing hardness values among batches (B1–B12) are associated with enhanced development of more effective compaction of the JLP, drug and other excipients, as depicted in Fig. 7(A). However, friability demonstrated a decreasing effect as the binder concentration increased, as shown in Fig. 7(B). The decrease in friability indicates the enhanced mechanical integrity of the tablets. Among the two variables, friability is the most important for binder selection, as it immediately indicates the tablet's capacity to endure handling and transportation. The optimum binder concentration was selected based on its capacity to achieve satisfactory hardness while maintaining friability below the Pharmacopoeial standards.

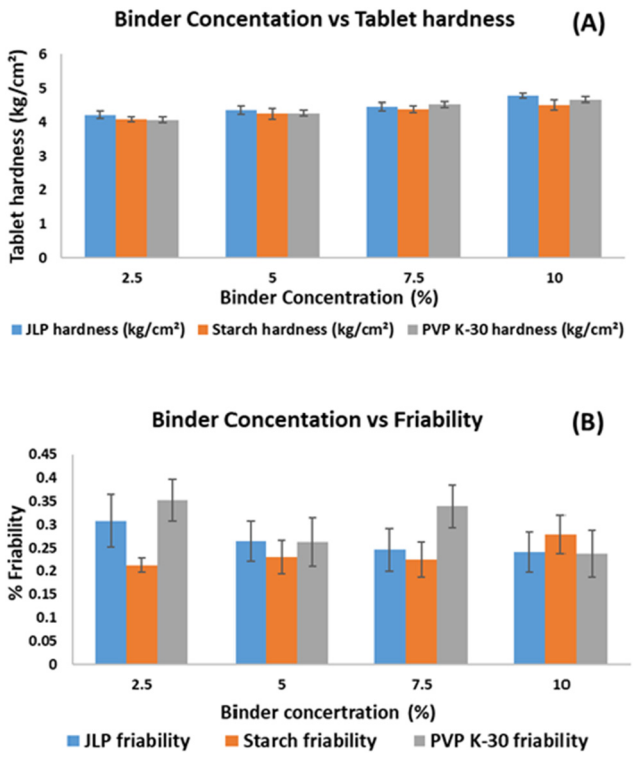

Fig. 7 Mechanical strength of tablets prepared using JLP as a binding agent: (A) binder concentration *vs.* tablet hardness and (B) binder concentration *vs.* friability.

Using a pH 7.5 phosphate buffer, the disintegration time of the formulated tablet batches was assessed. In formulation B1 through B4, the disintegration time increased gradually from 8.28 ± 0.361 (2.5% JLP) to 13.68 ± 0.44 min (10% JLP). Similarly, starch-based formulations (B5–B8) showed disintegration times from 5.31 ± 0.19 to 9.18 ± 0.512 minutes. The disintegration time of the PVP K-30-incorporated formulations (B9–B12) ranged from 5.57 ± 0.217 to 8.44 ± 0.384 minutes. According to Indian Pharmacopoeia, the disintegration time results lie within 15 minutes. A progressive increase in polymer concentration was found to increase the disintegration time in each formulation batch of tablets.[52]

3.3.2 *In vitro* dissolution study and release kinetics. The cumulative release of DS (as a percentage of drug release) for various formulation batches *versus* time is shown in Fig. 8. The curves (B1, B2, B3, and B4) represent the cumulative % release of DS from JLP-based matrix tablets. B1 (2.5% JLP) exhibited an initial burst release of the drug and a cumulative release of 87.35% after 45 minutes. Increasing the JLP concentration in B2 (5% JLP), B3 (7.5% JLP), and B4 (10% JLP) resulted in a gradual decrease in cumulative drug release, with values of 83.07%, 80.40%, and 77.75%, respectively, after 45 minutes. These release data suggest that a higher JLP content enhances the gel strength and viscosity of the matrix, slowing water penetration and drug diffusion. The values of T_{50}% and T_{90}% showed a gradual rise with increasing JLP concentrations. This could be explained by the potential that increased JLP concentrations may retard the dissolution process by delaying the disintegration of primary drug particles. Similar results were also

Open Access Article. Published on 12 January 2026. Downloaded on 3/17/2026 6:44:35 PM.
This article is licensed under a Creative Commons Attribution-NonCommercial 3.0 Unported Licence.

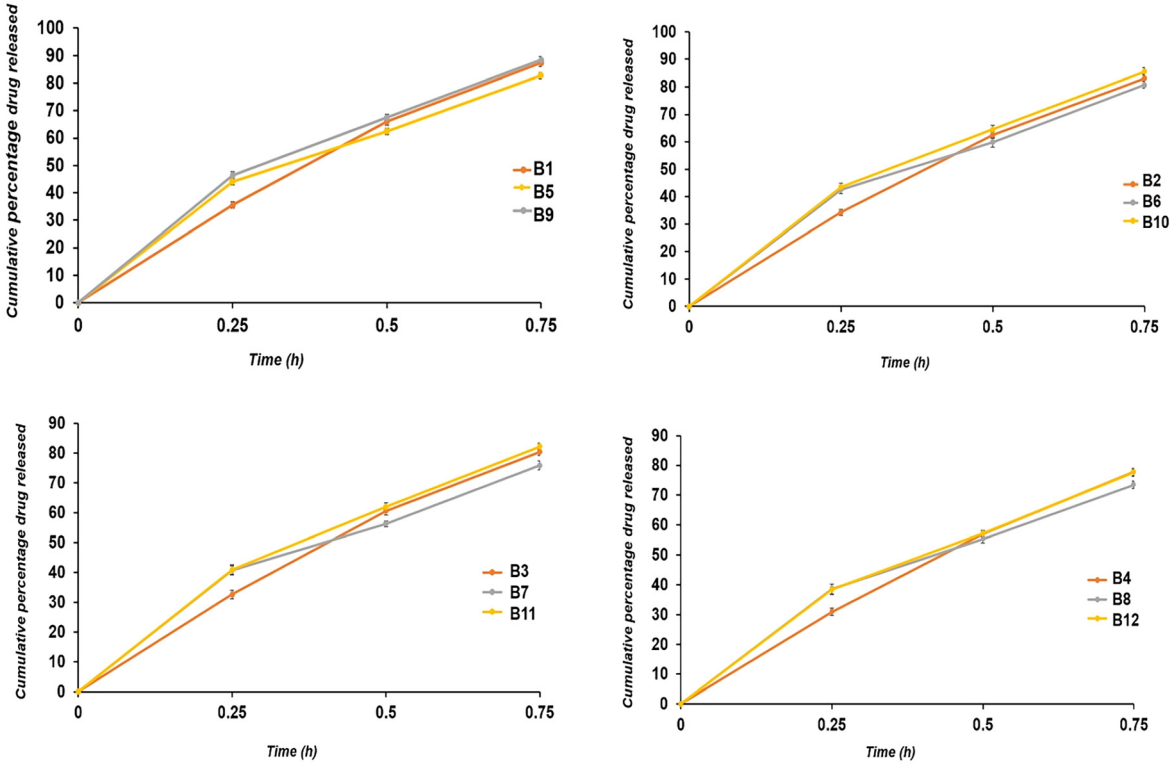

Fig. 8 Cumulative percentage of drug released at various time intervals from all tablet batches (B1 to B12).

observed for PVP K-30 and starch-based tablets. Similarly, Manna *et al.* observed a comparable dissolution pattern in DS tablets made with *Colocasia esculenta*.[8] The tablets composed of PVP K-30 showed relatively lower T_{50}%, which may be due to their high disintegrating ability. Drug release was relatively slower in the starch-based formulations (B5, B6, B7, and B8) with 2.5%, 5%, 7.5%, and 10% starch, respectively, than in the comparable JLP formulations. After 45 min, the cumulative release of DS varied from 82.71% for 2.5% starch to 73.50% for 10% starch. Conversely, the PVP K-30-based formulations (B9, B10, B11, and B12) containing 2.5%, 5%, 7.5%, and 10% PVP K-30 demonstrated a comparatively greater burst release of DS from the tablet matrix. This faster release could be attributed to the pronounced disintegrating effect of PVP K-30, which facilitates rapid matrix disintegration and drug diffusion. The cumulative drug release after 45 minutes for the PVP K-30 batches ranged from 88.47% to 77.60% depending on the polymer concentration.[53] For all the prepared formulations except B3, the highest R^2 values were obtained for the Higuchi model (0.9797–0.9999). This indicates that a diffusion-controlled process is followed as the primary mechanism of drug release from the prepared matrix tablets. B3 followed the Hixon Crowell model, representing drug release controlled by changes in the surface area and particle size of the dosage form during dissolution. The Korsmeyer–Peppas n values, ranging from around 0.56 to 0.84, indicate that most batches exhibit anomalous (non-Fickian) transport, signifying that drug release is influenced by both diffusion and polymer relaxation or erosion. Based on the regression coefficient (R^2) values obtained and displayed in Table 6, the drug release mechanism was predicted.[54]

3.3.4 Stability study. The results obtained after the accelerated stability study of the different parameters of tablets (batch B1) are illustrated in Table 7. The evaluation parameters of the tablet, including weight uniformity, drug content, hardness, and cumulative percent release (CPR) at 45 minutes, were evaluated for a storage time of 90 days. The weight uniformity of the tablets exhibited no variation during the evaluation period, indicating uniformity in their physical integrity. The initial drug content was 99.43%, which significantly decreased to 98.38% after 90 days, indicating minimal drug degradation during storage. The hardness values remained consistently unchanged (4.22–4.41 kg m^{-2}), indicating that the mechanical strength was not diminished during storage. The hardness values remained remarkably unaffected (4.22–4.41 kg m^{-2}), indicating that mechanical strength did not decrease during storage. The CPR at 45 minutes exhibited a gradual decrease from 87.35% on day 0 to 85.32% on day 90, demonstrating a variation of approximately 2.3% that is within the acceptable Pharmacopeial standards. The modifications in the dissolution profile were insignificant and were not indicative of considerable formulation instability. After three months of stability testing, there were no apparent modifications in the FTIR spectrum. This confirms the findings that the formulation exhibits good stability under the investigated conditions. The overall stability profile of batch B1 tablets

 © 2026 The Author(s). Published by the Royal Society of Chemistry

Open Access Article. Published on 12 January 2026. Downloaded on 3/17/2026 6:44:35 PM.
This article is licensed under a Creative Commons Attribution-NonCommercial 3.0 Unported Licence.

Table 6 Kinetics of drug release, including T_{50}%, T_{90}%, and CPR at 45 minutes for the prepared tablet batches

	Regression coefficients (R^2 value)								
					Korsmeyer–Peppas				
Batch no.	Zero order	First order	Higuchi	Hixon Crowell	R^2	N	T_{50}% (h)	T_{90}% (h)	CPR at 45 min
B1	0.995	0.9552	**0.9994**	0.9976	0.996	0.7813	0.36	0.78	87.352 ± 1.35
B2	0.9962	0.9568	**0.9998**	0.9984	0.996	0.8266	0.38	0.83	83.07 ± 1.65
B3	0.9951	0.9555	0.9995	**0.9997**	0.9961	0.8295	0.39	0.95	80.40 ± 1.104
B4	0.9966	0.9651	**0.9999**	0.9984	0.9986	0.844	0.42	0.93	77.75 ± 1.298
B5	0.9799	0.996	**0.9895**	0.9826	0.9925	0.5665	0.32	0.90	82.71 ± 1.09
B6	0.9811	0.9986	**0.9832**	0.9776	0.9875	0.5738	0.34	0.94	80.73 ± 1.21
B7	0.9793	0.9995	**0.9797**	0.9786	0.9837	0.5557	0.37	1.06	75.89 ± 1.52
B8	0.9812	0.9954	**0.99**	0.9896	0.9932	0.5799	0.40	1.05	73.50 ± 1.21
B9	0.9809	0.9914	**0.9945**	0.9823	0.9967	0.5812	0.29	0.79	88.47 ± 1.22
B10	0.9838	0.9907	**0.9944**	0.9853	0.9971	0.6106	0.56	0.91	85.58 ± 1.27
B11	0.9854	0.9883	**0.9958**	0.9902	0.9983	0.6306	0.59	0.94	82.21 ± 1.04
B12	0.9861	0.9946	**0.9895**	0.986	0.9941	0.6311	0.62	0.99	77.60 ± 1.21

Table 7 Various parameters evaluated during three months of accelerated stability study

	Batch B1 (JLP 2.5% w/w)			
Evaluation parameters	0 days	30 days	60 days	90 days
Weight uniformity (mg) (n = 20)	202.97 ± 1.955	201.94 ± 1.218	201.47 ± 1.203	202.86 ± 1.318
Drug content (%) (n = 10)	99.43 ± 0.373	98.92 ± 0.584	98.59 ± 0.618	98.38 ± 0.850
Hardness (kg m^{-2}) (n = 5)	4.22 ± 0.105	4.37 ± 0.135	4.32 ± 0.193	4.41 ± 0.215
$CPR_{45\ min}$ (n = 3)	87.352 ± 1.35	86.316 ± 1.76	86.021 ± 1.51	85.324 ± 1.98

remained unaltered by the slight decrease in drug content and dissolution efficiency, and no significant morphological or physicochemical modifications were observed throughout the 90-day accelerated stability analysis. Similar results were reported using taro stolon polysaccharide as a tablet binder.[8] FT-IR analysis was used to evaluate the chemical stability and

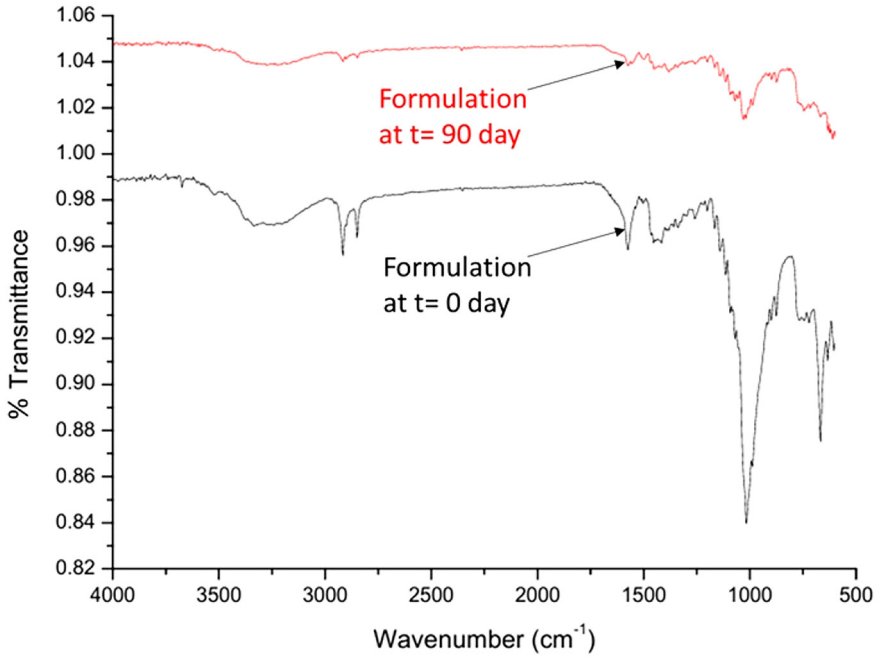

Fig. 9 FTIR spectra after accelerated stability study of DS-incorporated tablet formulation (B1 batch).

Open Access Article. Published on 12 January 2026. Downloaded on 3/17/2026 6:44:35 PM.
This article is licensed under a Creative Commons Attribution-NonCommercial 3.0 Unported Licence.

compatibility of diclofenac sodium with the JLP polymer and excipients under accelerated and real-time storage conditions (as shown in Fig. 9). In general, the peaks observed after 90 days of the accelerated stability study did not show any major deviations from the formulation IR spectra. The peak for the N–H or O–H band observed in pure diclofenac sodium was flattened to some extent, which could be due to the absorption of a trace amount of moisture within the tablet formulation at higher relative humidity during storage. The peak for C=O/C–O band (at 1574–1575 cm^{-1} in pure DS) was observed in the formulation after 90 days at 1568.61 cm^{-1}. The peak for the C–C ring band (1452 cm^{-1} in pure DS) was observed in the formulation after 90 days at 1442.96 cm^{-1}. The peak for C–N stretching (at 1305 cm^{-1} in pure DS) was observed in the formulation after 90 days at 1307.72 cm^{-1}. No additional peaks or complete elimination of the diagnostic bands were observed. The intensity IR peaks of the formulation are reduced after 90 days of storage conditions. This may have resulted from the gradual degradation of the formulation subjected to temperature and relative humidity. A minimal absorption of moisture might result in changes in peak intensity or the elimination of specific bands due to the development of hydrogen bonds or other polymorphism modifications.[23]

4. Conclusion

The present investigation reported the extraction and characterization of a novel JLP as a binding agent for the preparation of tablets. The extracted JLP was characterized for phytoconstituent screening, organoleptic properties, total polysaccharide content, ^{13}C solid-state NMR spectroscopy, elemental analysis, FTIR spectroscopy, molar mass, zeta potential, particle size, pH, surface tension, viscosity, and water solubility, swelling index, stability study in aqueous environment, DSC, TGA, DTA, powder X-ray diffraction, and scanning electron microscopy. The FTIR analysis and zeta potential value revealed the anionic behaviour of the polysaccharide. The molar mass and average zeta potential of JLP were reported to be 2.12 (±0.05) × 10^5 Da and −4.6 (±0.4) mV, respectively. The elemental analysis study report indicated the presence of carbon, hydrogen, sulphur and nitrogen. The XRD study indicated the amorphous nature of JLP. The FTIR and DSC study reports indicated compatibility between JLP and DS within the formulation. The prepared granules showed suitable behaviour and a compressible nature for tablet compression. The *in vitro* drug release data indicated a decreased cumulative percentage of drug release with an increasing JLP concentration. The release kinetic data showed that the majority of the formulations followed the Higuchi mechanism, demonstrating diffusion-controlled drug release from a relatively insoluble polymer matrix. The *n* value suggested a non-Fickian diffusion mechanism for releasing the drug from the polymer matrix. Even 2.5% w/w JLP concentration exhibited low percentage friability, required hardness and desirable drug release for conventional dosage forms of DS, reflecting the potential of JLP as a tablet binder. The obtained results established jute leaf polysaccharide as a safe and sustainable alternative to existing tablet binders.

Author contributions

Olivia Sen: writing – original draft, validation, resources, data curation, methodology, investigation, formal analysis. Devlina Pal: writing – review & editing, methodology, investigation, formal analysis, supervision. Tamal Jana: data curation, methodology, investigation. Sanchita Das: formal analysis, supervision. Gouranga Nandi: resources, methodology. Sreejan Manna: writing – original draft, writing – review & editing, conceptualization, supervision, resources, methodology.

Data availability

All the experimentally obtained data are included in the manuscript.

Conflicts of interest

The authors declare that they have no known competing financial interests or personal relationships that could have appeared to influence the work reported in this paper.

Acknowledgements

The research did not receive any specific grant from funding agencies in the public, commercial, or not-for-profit sectors. The authors are extremely grateful to the authority of JIS University, Brainware University, B.C.D.A. College of Pharmacy & Technology and University of North Bengal for providing the required facilities to complete this study.

References

1 T. A. Moges, F. N. Dagnew, W. S. Zewdu, A. N. Assefa, Y. A. Ferede, M. A. Ayicheh and S. B. Dagnew, The impact of patients' preference for pharmaceutical dosage forms on medication discontinuation among patients attending Red Cross pharmacies in Northwest Ethiopia, *Sci. Rep.*, 2024, **14**(1), 28751, DOI: 10.1038/s41598-024-76113-6.
2 T. P. Forbes, O. Agolini, Z. Altamimi and J. Lawrence, Personalized Medicine: A Quality by Design Approach to Printable Tablet Production, *RSC Pharm.*, 2025, **2**, 1096–1109, DOI: 10.1039/D5PM00041F.
3 M. S. Arshad, S. Zafar, B. Yousef, Y. Alyassin, R. Ali, A. AlAsiri, M. W. Chang, Z. Ahmad, A. A. Elkordy, A. Faheem and K. Pitt, A review of emerging technologies enabling improved solid oral dosage form manufacturing and processing, *Adv. Drug Delivery Rev.*, 2021, **178**, 113840, DOI: 10.1016/j.addr.2021.113840.

 © 2026 The Author(s). Published by the Royal Society of Chemistry

Open Access Article. Published on 12 January 2026. Downloaded on 3/17/2026 6:44:35 PM.
This article is licensed under a Creative Commons Attribution-NonCommercial 3.0 Unported Licence.

4 E. Franceschinis, V. Bressan, E. Fontanel, N. Realdon, S. Volpato and A. C. Santomaso, Effect of the drying type on the properties of granules and tablets produced by high shear wet granulation, *Powder Technol.*, 2024, **434**, 119316, DOI: 10.1016/j.powtec.2023.119316.
5 A. Abaci, C. Gedeon, A. Kuna and M. Guvendiren, Additive manufacturing of oral tablets: technologies, materials and printed tablets, *Pharmaceutics*, 2021, **13**(2), 156, DOI: 10.3390/pharmaceutics13020156.
6 L. R. Sanjay, M. K. Ashokbhai, S. Ghatole, S. Roy, K. P. Kashinath and S. Kaity, Strategies for beating bitter taste of pharmaceutical formulations towards better therapeutic outcome, *RSC Pharm.*, 2025, **2**, 59–81, DOI: 10.1039/D4PM00191E.
7 D. Das, S. M. K. Das, T. Jamatia, B. Bhattacharya, R. Mazumder, P. K. Yadav, N. R. Bishwas, T. Deka, D. Roy, B. Sinha and B. Das, Advances of cassava starch-based composites in novel and conventional drug delivery systems: a state-of-the-art review, *RSC Pharm.*, 2024, **1**, 182–203, DOI: 10.1039/D3PM00008G.
8 S. Manna, S. Sarkar, R. Sahu, T. K. Dua, P. Paul, S. Jana and G. Nandi, Characterization of Taro (Colocasia esculenta) stolon polysaccharide and evaluation of its potential as a tablet binder in the formulation of matrix tablet, *Int. J. Biol. Macromol.*, 2024, **280**, 135901, DOI: 10.1016/j.ijbiomac.2024.135901.
9 S. B. Dhull, P. Bamal, M. Kumar, S. P. Bangar, P. Chawla, A. Singh, W. Mushtaq, M. Ahmad and S. Sihag, Fenugreek (Trigonella foenum graecum) gum: A functional ingredient with promising properties and applications in food and pharmaceuticals—A review, *Legume Sci.*, 2023, **5**(3), e176, DOI: 10.1002/leg3.176.
10 S. Manna, S. Karmakar, O. Sen, P. Sinha, S. Jana and S. Jana, Recent updates on guar gum derivatives in colon specific drug delivery, *Carbohydr. Polym.*, 2024, **334**, 122009, DOI: 10.1016/j.carbpol.2024.122009.
11 N. Amjed, M. Zeshan, A. Farooq and S. Naz, Applications of guar gum polysaccharide for pharmaceutical drug delivery: a review, *Int. J. Biol. Macromol.*, 2024, **257**, 128390, DOI: 10.1016/j.ijbiomac.2023.128390.
12 M. Ramesh and C. Deepa, Processing and properties of jute (Corchorus olitorius L.) fibres and their sustainable composite materials: a review, *J. Mater. Chem. A*, 2024, **12**(4), 1923–1997, DOI: 10.1039/D3TA05481K.
13 P. M. Afokpe, S. Ologou, S. R. Kouiho, S. J. de Hoop, S. N'Danikou, E. G. Achigan-Dako and M. E. Schranz, Unveiling genetic diversity in jute mallow (Corchorus spp.): morphological clustering reveals distinctive traits among accessions from Africa and Asia, *Genet. Resour. Crop Evol.*, 2024, 1–23, DOI: 10.1007/s10722-024-02295-7.
14 J. Tang, X. Qin, R. Repo-Carrasco-Valencia, X. Yang, Y. Deng, C. Hou and X. Yang, Physicochemical, functional and antioxidant properties of four polysaccharides sequentially extracted from jute (Corchorus olitorius L.) leaves, *Int. J. Biol. Macromol.*, 2025, 147223, DOI: 10.1016/j.ijbiomac.2025.147223.
15 M. A. Shewaiter, T. M. Hammady, A. El-Gindy, S. H. Hammadi and S. Gad, Formulation and characterization of leflunomide/diclofenac sodium microemulsion base-gel for the transdermal treatment of inflammatory joint diseases, *J. Drug Delivery Sci. Technol.*, 2021, **61**, 102110, DOI: 10.1016/j.jddst.2020.102110.
16 Y. Zhang, D. Yang, B. Shuai, H. Ding, J. Yang, J. Wang, L. Tang and S. Yao, Diclofenac sodium nanomedicine results in pain-relief and differential expression of the RNA transcriptome in the spinal cord of SNI rats, *Int. J. Pharm.*, 2024, **659**, 124276, DOI: 10.1016/j.ijpharm.2024.124276.
17 M. N. Sarwar, A. Ullah, M. K. Haider, N. Hussain, S. Ullah, M. Hashmi, M. Q. Khan and I. S. Kim, Evaluating antibacterial efficacy and biocompatibility of PAN nanofibers loaded with diclofenac sodium salt, *Polymers*, 2021, **13**(4), 510, DOI: 10.3390/polym13040510.
18 S. Oh and D. Y. Kim, Characterization, antioxidant activities, and functional properties of mucilage extracted from Corchorus olitorius L., *Polymers*, 2022, **14**(12), 2488, DOI: 10.3390/polym14122488.
19 H. Huojiaaihemaiti, P. Mutaillifu, A. Omer, R. Nuerxiati, X. Duan, X. Xin and A. Yili, Isolation, structural characterization, and biological activity of the two acidic polysaccharides from the fruits of the Elaeagnus angustifolia Linnaeus, *Molecules*, 2022, **27**(19), 6415, DOI: 10.3390/molecules27196415.
20 A. Gizaw, L. M. Marami, I. Teshome, E. J. Sarba, P. Admasu, D. A. Babele, G. M. Dilba, W. M. Bune, M. D. Bayu, M. Tadesse and K. Abdisa, Phytochemical screening and in vitro antifungal activity of selected medicinal plants against Candida albicans and Aspergillus niger in West Shewa Zone, Ethiopia, *Adv. Pharmacol. Pharm. Sci.*, 2022, 3299146, DOI: 10.1155/2022/3299146.
21 A. Hassan, Z. Akmal and N. Khan, The phytochemical screening and antioxidants potential of Schoenoplectustriqueter L. Palla, *J. Chem.*, 2020, **2020**(1), 3865139, DOI: 10.1155/2020/3865139.
22 S. Y. Li, C. Q. Duan and Z. H. Han, Grape polysaccharides: compositional changes in grapes and wines, possible effects on wine organoleptic properties, and practical control during winemaking, *Crit. Rev. Food Sci. Nutr.*, 2023, **63**(8), 1119–1142, DOI: 10.1080/10408398.2021.1960476.
23 S. Sarkar, S. Manna, E. Das, P. Jana, S. Mukherjee, R. Sahu, T. K. Dua, P. Paul, S. Kaity and G. Nandi, Fabrication and optimization of extended-release beads of diclofenac sodium based on Ca^{2+} cross-linked Taro (Colocasia esculenta) stolon polysaccharide and pectin by quality-by-design approach, *Int. J. Biol. Macromol.*, 2024, **271**, 132606, DOI: 10.1016/j.ijbiomac.2024.132606.
24 A. Changder, R. Paul, A. Ghosh, S. Sarkar, G. Nandi and L. K. Ghosh, Grafting of poly(acrylic acid) onto Cassia fistula seed gum: synthesis, optimization, and characterization, *Int. J. Pharm. Sci. Nanotechnol.*, 2023, **16**(1), 6294–6308, DOI: 10.37285/ijpsn.2023.16.1.4.
25 S. Patra, N. N. Bala and G. Nandi, Synthesis, characterization and fabrication of sodium carboxymethyl-okra-gum-

Open Access Article. Published on 12 January 2026. Downloaded on 3/17/2026 6:44:35 PM.
This article is licensed under a Creative Commons Attribution-NonCommercial 3.0 Unported Licence.

grafted-polymethacrylamide into sustained release tablet matrix, *Int. J. Biol. Macromol.*, 2020, **164**, 3885–3900, DOI: 10.1016/j.ijbiomac.2020.09.025.

26 A. Changder, S. K. Mandal, S. Sarkar, R. Paul, A. Ghosh, P. Paul, T. K. Dua, R. Sahu, G. Nandi and L. K. Ghosh, Evaluation of Cassia fistula seed galactomannan as tablet-binder in formulation of diclofenac sodium-loaded monolithic matrix tablet, *Int. J. Biol. Macromol.*, 2023, **253**, 127173, DOI: 10.1016/j.ijbiomac.2023.127173.

27 R. Malviya, S. Sundram, S. Fuloria, V. Subramaniyan, K. V. Sathasivam, A. K. Azad, M. Sekar, D. H. Kumar, S. Chakravarthi, O. Porwal and D. U. Meenakshi, Evaluation and characterization of tamarind gum polysaccharide: the biopolymer, *Polymers*, 2021, **13**(18), 3023, DOI: 10.3390/molecules28186477.

28 World Health Organization, *Quality Control Methods for Medicinal Plant Materials*, WHO, Geneva, 2025, available at: https://www.who.int/docs/default-source/medicines/norms-and-standards/guidelines/quality-control/quality-control-methods-for-medicinal-plant-materials.pdf?sfvrsn=b451e7c6_0 (accessed Sept 18, 2025).

29 K. Bu, Y. Wang, C. Du, W. Chu, L. Xing, X. Wang, H. Lin and P. Wang, Effects of different extraction procedures on textural, rheological, and swelling properties of Ulva clathrata polysaccharide hydrogels, *Int. J. Biol. Macromol.*, 2025, 144086, DOI: 10.1016/j.ijbiomac.2025.144086.

30 G. Jebeso, D. Gebeyehu and M. Abere, Characteristics and quality of gum arabic derived from naturally grown *Acacia seyal* Willdenow tree in the lowland areas of Ethiopia, *Food Chem. Adv.*, 2023, **2**, 100243, DOI: 10.1016/j.focha.2023.100243.

31 A. Sharma and K. J. Kumar, Preparation, structural and rheological evaluation of multifunctional premix using *Butea monosperma* gum in combination with edible gums: A concentration-dependent study, *Int. J. Biol. Macromol.*, 2025, 145126, DOI: 10.1016/j.ijbiomac.2025.145126.

32 C. Malsawmtluangi, K. Thanzami, H. Lalhlenmawia, V. Selvan, S. Palanisamy, R. Kandasamy and L. Pachuau, Physicochemical characteristics and antioxidant activity of *Prunus cerasoides* D. Don gum exudates, *Int. J. Biol. Macromol.*, 2014, **69**, 192–199, DOI: 10.1016/j.ijbiomac.2014.05.050.

33 S. Pradhan, A. Roy, A. Saha, P. Das, G. J. Ashraf, T. Baishya, A. Thapa, T. K. Dua, P. Paul, G. Nandi and P. P. Maiti, Bioinspired synthesis of silver nanoparticles using *Luffa aegyptiaca* seed extract and assessment of pharmacological properties, *Biocatal. Agric. Biotechnol.*, 2024, **58**, 103209, DOI: 10.1016/j.bcab.2024.103209.

34 A. E. Kassa, N. T. Shibeshi and B. Z. Tizazu, Kinetic analysis of aluminum extraction from Ethiopian kaolinite using hydrochloric acid, *Int. J. Chem. Eng.*, 2022, **2022**(1), 2292814, DOI: 10.1155/2022/2292814.

35 M. A. Thakar, S. S. Jha, K. Phasinam, R. Manne, Y. Qureshi and V. H. Babu, X-ray diffraction (XRD) analysis and evaluation of antioxidant activity of copper oxide nanoparticles synthesized from leaf extract of Cissus vitiginea, *Mater. Today: Proc.*, 2022, **51**, 319–324, DOI: 10.1016/j.matpr.2021.05.410.

36 A. Madaci, H. Ferkous, A. Sedik, A. Delimi, C. Boulechfar, A. Belakhdar, M. Berredjem, M. A. Chaouch, M. Alam, H. Majdoub and N. Jaffrezic-Renault, Experimental and theoretical study of polysaccharides extracted from prickly pear nopales pulp (PPUN) of Opuntia ficus-indica as corrosion inhibitors, *J. Mol. Liq.*, 2023, **384**, 122272, DOI: 10.1016/j.molliq.2023.122272.

37 K. Gowthamarajan, G. K. Kumar, N. B. Gaikwad and B. Suresh, Preliminary study of Anacardium occidentale gum as binder in formulation of paracetamol tablets, *Carbohydr. Polym.*, 2011, **83**(2), 506–511, DOI: 10.1016/j.carbpol.2010.08.010.

38 L. Gallo, M. V. Ramírez-Rigo, J. Piña and V. Bucalá, A comparative study of spray-dried medicinal plant aqueous extracts: drying performance and product quality, *Chem. Eng. Res. Des.*, 2015, **104**, 681–694, DOI: 10.1016/j.cherd.2015.10.009.

39 S. Singh, G. D. Dadabhau and K. Singh, Formulation, development and investigation of matrix type sustained release tablet of antiulcer drug by using soluble polymer as a drug release retarding agent, *Int. J. Membr. Sci. Technol.*, 2023, **10**(4), 2593–2603, DOI: 10.15379/ijmst.v10i4.3701.

40 M. Butola, A. Badola, N. Nainwal, S. Rana, V. Jakhmola, Y. Ale and A. N. Ansori, Formulation of sustained-release tablets of tolperisone HCl using different blends of hydrophilic and hydrophobic polymers, *Indian J. Pharm. Educ. Res.*, 2024, **58**(3s), s872–s879.

41 S. S. Gaikwad and S. J. Kshirsagar, Application of tablet-in-tablet technique to design and characterize immediate and modified release tablets of timolol maleate, *Heliyon*, 2024, **10**(3), e25820, DOI: 10.1016/j.heliyon.2024.e25820.

42 S. A. Nangare, A. H. Ali, K. R. Mahadik and S. S. Patil, Fabrication, optimization and characterization of an osmotic push-pull drug delivery system for paliperidone, *J. Taibah Univ. Med. Sci.*, 2023, **18**(6), 1511–1518, DOI: 10.1016/j.jtumed.2023.08.002.

43 D. G. Dastidar, A. Biswas, A. Das, S. Naskar and R. Mahish, Development and optimization of sustained-release matrix tablets of diclofenac sodium using carboxymethylated chitosan through systematic application of design of experiments, *Drug Metab. Bioanal. Lett.*, 2024, **17**(3), 121–136, DOI: 10.2174/0118723128351869250213102431.

44 A. Nagarsheth, D. Patel and H. Thakkar, Formulation and evaluation of proliposomal tablet of diclofenac sodium, *J. Drug Delivery Sci. Technol.*, 2022, **71**, 103353, DOI: 10.1016/j.jddst.2022.103353.

45 S. Salunkhe, G. Singh and H. Kaur, Evaluation of secondary metabolites and antimicrobial activity of herbal syrups of different brands, *Int. J. Sci. Res. Sci. Technol.*, 2025, **12**(4), 62–70, DOI: 10.32628/IJSRST251251.

46 R. Guo, N. Cao, Y. Wu and J. Wu, Optimized extraction and molecular characterization of polysaccharides from Sophora alopecuroides L. seeds, *Int. J. Biol. Macromol.*, 2016, **82**, 231–242, DOI: 10.1016/j.ijbiomac.2015.10.002.

 © 2026 The Author(s). Published by the Royal Society of Chemistry

Open Access Article. Published on 12 January 2026. Downloaded on 3/17/2026 6:44:35 PM.
This article is licensed under a Creative Commons Attribution-NonCommercial 3.0 Unported Licence.

47 Y. Wang, Y. Li, Y. Liu, X. Chen and X. Wei, Extraction, characterization and antioxidant activities of Se-enriched tea polysaccharides, *Int. J. Biol. Macromol.*, 2015, **77**, 76–84, DOI: 10.1016/j.ijbiomac.2015.02.052.

48 W. Tang, C. Liu, J. Liu, L. Hu, Y. Huang, L. Yuan, F. Liu, S. Pan, S. Chen, S. Bian and X. Huang, Purification of polysaccharide from Lentinus edodes water extract by membrane separation and its chemical composition and structure characterization, *Food Hydrocolloids*, 2020, **105**, 105851, DOI: 10.1016/j.foodhyd.2020.105851.

49 C. Mircioiu, V. Voicu, V. Anuta, A. Tudose, C. Celia, D. Paolino, M. Fresta, R. Sandulovici and I. Mircioiu, Mathematical modeling of release kinetics from supramolecular drug delivery systems, *Pharmaceutics*, 2019, **11**(3), 140, DOI: 10.3390/pharmaceutics11030140.

50 F. O. Ohwoavworhua and T. A. Adelakun, Some physical characteristics of microcrystalline cellulose obtained from raw cotton of Cochlospermumplanchonii, *Trop. J. Pharm. Res.*, 2005, **4**(2), 501–507, DOI: 10.4314/tjpr.v4i2.14626.

51 M. Ahuja, A. Kumar, P. Yadav and K. Singh, Mimosa pudica seed mucilage: Isolation; characterization and evaluation as tablet disintegrant and binder, *Int. J. Biol. Macromol.*, 2013, **57**, 105–110, DOI: 10.1016/j.ijbiomac.2013.03.004.

52 B. Asrade, E. Tessema and A. Tarekegn, In vitro comparative quality evaluation of different brands of carbamazepine tablets commercially available in Dessie town, Northeast Ethiopia, *BMC Pharmacol. Toxicol.*, 2023, **24**(35), DOI: 10.1186/s40360-023-00670-1.

53 A. S. Lourenco, T. Schuster, J. A. Lopes and A. Kirsch, A non-linear modelling approach to predict the dissolution profile of extended-release tablets, *Eur. J. Pharm. Sci.*, 2025, **204**, 106976, DOI: 10.1016/j.ejps.2024.106976.

54 A. S. Sousa, J. Serra, C. Estevens, R. Costa and A. J. Ribeiro, A comparative study of two data-driven modeling approaches to predict drug release from ER matrix tablets, *Int. J. Pharm.*, 2025, **671**, 125230, DOI: 10.1016/j.ijpharm.2025.125230.